Organometallics **1982,** *1,* 1437-1443 1437

Synthesis and Characterization of Phosphido-Bridged Fe_2Rh Clusters. Crystal and Molecular Structure of $Fe_2Rh(\mu\text{-}PPh_2)_3(CO)_6(PPh_3)$

Michael J. Breen and Gregory L. Geoffroy*

Department of Chemistry, The Pennsylvania State University, University Park, Pennsylvania 16802

Received July 19, 1982

The reaction of $Li[Fe_2(\mu\text{-}PPh_2)_2(CO)_5PPh_2]$ with *trans*-$RhCl(CO)(PR_3)_2$ (R = Et, Ph) yields the new phosphido-bridged clusters $Fe_2Rh(\mu\text{-}PPh_2)_3(CO)_6(PR_3)$. These compounds have been characterized spectroscopically, and $Fe_2Rh(\mu\text{-}PPh_2)_3(CO)_6(PPh_3)$ has been characterized by a complete single-crystal X-ray diffraction study. It crystallizes in the monoclinic space group $P2_1/c$ with a = 14.062 (9) Å, b = 21.212 (8) Å, c = 19.164 (6) Å, β = 109.22 (4)°, V = 5397 (9) Å^3, and Z = 4. Diffraction data ($3.0° \leq 2\theta \leq 50°$) were collected with an Enraf-Nonius CAD4 automated diffractometer, using graphite-monochromatized Mo Kα radiation, and the structure was refined to R = 0.051 and R_w = 0.057 for the 6818 independent reflections with $I \geq 3.0\ \sigma(I)$. The cluster has a closed triangular arrangement of metal atoms with each metal-metal bond bridged by a μ-PPh_2 ligand. One Fe-Rh bond is additionally bridged by a carbonyl ligand, and the Fe is further coordinated by two terminal CO's. The other Fe is ligated by three CO's and the Rh by PPh_3. Both Fe_2Rh complexes react with CO to displace the PR_3 ligand and add two CO's to form $Fe_2Rh(\mu\text{-}PPh_2)_3(CO)_8$. Upon heating under vacuum this species loses CO to generate $Fe_2Rh(\mu\text{-}PPh_2)_3(CO)_6$.

Although numerous metal carbonyl clusters have been prepared and studied, nearly all are coordinatively-saturated and without readily dissociable ligands.[1] Also, many show a marked tendency to fragment and rearrange under reaction conditions, in some cases destroying their polynuclear character.[1,2] Both properties are particularly undesirable if such polynuclear compounds are to be used as catalysts.[3] To properly assess the true potential for polynuclear catalysis a need exists for the preparation of new compounds which are either coordinatively unsaturated or which possess easily dissociable ligands and which have bridging ligands to retard fragmentation reactions.[4]

We have set out to prepare a series of such compounds which contain low-valent Rh(I) and Ir(I) centers linked to other metals via bridging phosphido ligands (μ-PR_2).[5] These metals appear ideal because of their demonstrated facility for addition and oxidative addition chemistry and the known utility of Rh(I) complexes in homogeneous catalysis.[6] Phosphido ligands are attractive because they resemble the ubiquitous PR_3 ligands found in many mononuclear catalysts, and they have been demonstrated to retard fragmentation reactions in many of their complexes.[7] Herein we report the synthesis and characterization of a series of phosphido-bridged trinuclear clusters which contain Rh(I) linked to two Fe centers.

Experimental Section

$Fe_2(\mu\text{-}PPh_2)_2(CO)_6$,[8] $Na_2[Fe_2(\mu\text{-}PPh_2)_2(CO)_6]$,[8] *trans*-$RhCl(CO)(PPh_3)_2$,[9] and *trans*-$RhCl(CO)(PEt_3)_2$[10] were prepared by literature procedures. PPh_2H and PPh_2Cl were obtained from Strem Chemicals Co. and used without further purification. All operations were carried out under an atmosphere of dry N_2, and all solvents were rigorously dried and deoxygenated prior to use. NMR spectra were recorded on a Bruker WP-200 FT NMR spectrometer. All reported ^{13}C NMR chemical shifts are relative to Me_4Si. $Cr(acac)_3$ (0.01 mol/mol of cluster) was added to each ^{13}C NMR sample as a shiftless relaxation agent.[11] ^{31}P NMR chemical shifts are relative to external 85% H_3PO_4 with downfield chemical shifts reported as positive. Electron-impact mass spectra were recorded on an AEI-MS9 mass spectrometer operated in the electron-impact mode with a source voltage of 70 eV and probe temperatures in the 100-200 °C range.

Preparation of $Fe_2(\mu\text{-}PPh_2)_2(CO)_5(PPh_2H)$, 1. Method A. A tetrahydrofuran (THF, 15 mL) solution of PPh_2Cl (0.18 mL, 0.22 g, 1.0 mmol) was added dropwise to a THF (50 mL) solution of $Na_2[Fe_2(\mu\text{-}PPh_2)_2(CO)_6]$ maintained at -78 °C by a dry ice/acetone slush bath. The latter was prepared in situ by the reduction of $Fe_2(\mu\text{-}PPh_2)_2(CO)_6$ (0.325 g, 0.5 mmol) with sodium.[8] The reaction mixture was slowly warmed to room temperature and stirred for several hours. THF was removed in vacuo and hexane (150 mL) added. After the mixture was filtered, the hexane-soluble material was chromatographed on silica gel with 1:4 CH_2Cl_2/hexane as eluant. Yellow, orange, and orange fractions of $Fe_2(\mu\text{-}PPh_2)_2(CO)_6$, $Fe_2(\mu\text{-}PPh_2)_2(CO)_5(PPh_2H)$, 1, and $Fe_2(\mu\text{-}PPh_2)_2(CO)_4(PPh_2H)_2$, 2, eluted in that order. The latter two compounds were obtained in 8.1% (0.033 g, 0.041 mmol) and 2.1% (0.010 g, 0.010 mmol) yields, respectively. The PPh_2H derivatives apparently form via the reaction of anionic PPh_2-substituted complexes with adventitious H_2O. Anal. Calcd for $C_{41}H_{31}Fe_2O_5P_3$, 1: C, 60.89; H, 3.84; Fe, 13.86. Found: C, 60.62; H, 4.18; Fe, 13,23.

1: IR ν_{CO}(hexane) 2028 (s), 1988 (s), 1965 (m), 1950 (s), 1925 (m) cm^{-1}; $^{31}P\{^1H\}$ NMR (25 °C, benzene-d_6) δ 145.9 (s), 51.3 (s); mass spectrum, m/e 808 (M^+), 780 ($M^+ - CO$), 752 ($M^+ - 2CO$), 724 ($M^+ - 3CO$), 696 ($M^+ - 4CO$), and 668 ($M - 5CO$).

---

[1] (a) Johnson, B. F. G., Ed. "Metal Clusters"; Wiley: New York, 1980. (b) Roberts, D. A.; Geoffroy, G. L. In "Comprehensive Organometallic Chemistry"; Wilkinson, G., Stone, F. G. A., Abels, E., Eds.; Pergamon Press: London, 1982; Chapter 40. (c) Gladfelter, W. L.; Geoffroy, G. L. *Adv. Organomet. Chem.* **1980**, *18*, 207. (d) Chini, P.; Heaton, B. T. *Top. Curr. Chem.* **1977**, *71*, 1. (e) Chini, P.; Longoni, G.; Albano, V. G. *Adv. Organomet. Chem.* **1976**, *14*, 285.

[2] Fox, J. R.; Gladfelter, W. L.; Geoffroy, G. L. *Inorg. Chem.* **1980**, *19*, 2574.

[3] Wyman, R. Chapter 8 in ref 1a.

[4] Progress has been made in this area. See: (a) Sivak, A. J.; Muetterties, E. L. *J. Am. Chem. Soc.* **1979**, *101*, 4878. (b) Fryzuk, M. D. *Organometallics* **1982**, *1*, 408.

[5] Breen, M. J.; Duttera, M. R.; Geoffroy, G. L.; Novotnak, G. C.; Roberts, D. A.; Shulman, P. M.; Steinmetz, G. R. *Organometallics* **1982**, *1*, 1008

[6] Parshall, G. W. "Homogeneous Catalysis";; Wiley: New York, 1980.

[7] (a) Carty, A. J.; Hartstock, F.; Taylor, N. J. *Inorg. Chem.* **1982**, *21*, 1349. (b) Carty, A. J. *Adv. Chem. Ser.* **1982**, *No. 196*, 163. (c) Finke, R. G.; Gaughan, G.; Pierpont, C.; Cass, M. E. *J. Am. Chem. Soc.* **1981**, *103*, 1394 and references cited therein. (d) Huttner, G.; Schneider, J.; Müller, H. D.; Mohr, G.; von Seyerl, J.; Wolfahrt, L. *Angew. Chem., Int. Ed. Engl.* **1979**, *18*, 76. (e) Werner, H.; Hofmann, W. *Ibid.* **1979**, *18*, 158. (f) Beurich, H.; Madach, T.; Richter, F.; Vahrenkamp, H. *Ibid.* **1979**, *18*, 690. (g) Vahrenkamp, H. *Ibid.* **1978**, *17*, 379.

[8] Collman, J. P.; Rothrock, R. K.; Finke, R. G.; Rose-Munch, F. *J. Am. Chem. Soc.* **1977**, *99*, 7381.

[9] Evans, D.; Osborn, J. A.; Wilkinson, G. *Inorg. Synth.* **1968**, *11*, 99.

[10] The procedure in ref 9 was utilized employing PEt_3 to prepare $RhCl(CO)(PEt_3)_2$.

[11] Gansow, O. A.; Burke, A. R.; La Mar, G. N. *J. Chem. Soc., Chem. Commun.* **1972**, 456.

0276-7333/82/2301-1437\$01.25/0

2: IR ν_{CO}(hexane) 2029 (s), 1975 (s), 1958 (s), 1946 (m), 1903 (m) cm^{-1}; $^{31}P\{^1H\}$ NMR (25 °C, benzene-d_6) δ 135.7 (t, $J_{^{31}P-^{31}P}$ = 13.7 Hz), 54.3 (t, $J_{^{31}P-^{31}P}$ = 13.7 Hz).

Method B. PhLi (1.85 M, 0.090 mL, 0.166 mmol) was added via syringe to a THF solution (20 mL) of $Fe_2(\mu\text{-}PPh_2)_2(CO)_6$ (0.100 g, 0.153 mmol) at 25 °C. After the resultant red solution had been stirred for 30 min, PPh_2H (0.027 mL, 0.029 g, 0.155 mmol) was added via syringe. Stirring was continued for 30 min, and glacial acetic acid (0.020 mL, 0.348 mmol) was added via syringe. The orange solution was stirred for 15 min and the THF removed in vacuo. Chromatography as above gave **1** in 92.8% yield (0.115 g, 0.142 mmol).

Method C. A hexane solution (50 mL) of $Fe_2(\mu\text{-}PPh_2)_2(CO)_6$ (1.03 g, 1.59 mmol) and PPh_2H (0.55 mL, 0.59 g, 3.16 mmol) was irradiated at 366 nm for 2 h. The solution was filtered and chromatographed as above, yielding **1** in 19.5% yield (0.25 g, 0.31 mmol).

Preparation of Solutions of $Li[Fe_2(\mu\text{-}PPh_2)_2(CO)_5(PPh_2)]$, 3. *n*-BuLi was added via syringe to a rigorously dried and deoxygenated THF solution of **1**. The initially orange solution immediately turned deep red as **3** was formed. **3** could not be isolated as a solid and was therefore utilized in situ: IR ν_{CO}(THF) 1995 (s), 1940 (vs, br), 1910 (s), 1883 (m), 1855 (sh) cm^{-1}; $^{31}P\{^1H\}$ NMR (25 °C, THF-d_8) δ 138.2 (d, $J_{^{31}P-^{31}P}$ = 8.7 Hz), 66.5 (t, $J_{^{31}P-^{31}P}$ = 8.7 Hz).

Preparation of $Fe_2Rh(\mu\text{-}PPh_2)_3(CO)_6(PEt_3)$, 4a. *n*-BuLi (0.51 mL of a 1.7 M solution, 0.867 mmol) in hexane was added to a THF solution (50 mL) of **1** (0.700 g, 0.866 mmol) to generate **3** in situ. This solution was slowly added with stirring to a THF solution of *trans*-$RhCl(CO)(PEt_3)_2$ (0.314 g, 0.78 mmol). After the solution was stirred at 25 °C for 18 h, the solvent was removed in vacuo and the product extracted with hexane. Hexane was removed in vacuo and the product washed with small aliquots of hexane to remove excess **1**. The green solid (0.50 g) which remained was largely **4a** but contained a small amount of **1** (<10%). It was recrystallized from petroleum ether by cooling to 0 °C to give a pure sample of **4a**: IR ν_{CO}(KBr) 2022 (s), 1984 (s), 1965 (m), 1942 (s), 1932 (s), 1781 (m) cm^{-1}; $^{31}P\{^1H\}$ NMR (−40 °C, toluene-d_8) δ 212.7 (dd, $J_{^{31}P-^{31}P}$ = 19.8 and 42.7 Hz), 141.5 (ddd, $J_{^{31}P-^{103}Rh}$ = 120.5 Hz, $J_{^{31}P-^{31}P}$ = 207.5 and 15.2 Hz), 114.7 (dddd, $J_{^{31}P-^{103}Rh}$ = 99.2 Hz, $J_{^{31}P-^{31}P}$ = 14.5, 42.7, and 207.5 Hz), 26.5 (dddd, $J_{^{31}P-^{103}Rh}$ = 213.6 Hz, $J_{^{31}P-^{31}P}$ = 19.8, 15.2, and 14.5 Hz). Anal. Calcd for $C_{48}H_{45}Fe_2O_6P_4Rh$: C, 54.57; H, 4.29; Fe, 10.57. Found: C, 54.86; H, 4.91; Fe, 10.26.

Preparation of $Fe_2Rh(\mu\text{-}PPh_2)_3(CO)_6(PPh_3)$, 4b. *n*-BuLi in hexane (0.177 mL, 1.7 M) was added via syringe to a THF solution (50 mL) containing **1** (0.244 g, 0.301 mmol) and *trans*-$RhCl(CO)(PPh_3)$ (0.160 g, 0.232 mmol). The solution was stirred for 2.5 h and the solvent removed in vacuo. The solids were extracted with three 10-mL aliquots of benzene and filtered through Celite 545. The benzene extracts were combined, and the solvent was removed in vacuo. The solid was washed three times with 10-mL aliquots of hexane to remove excess **1**. The remaining dark green solid (0.211 g) is primarily **4b** with a small amount of **1** impurity. Crystallization can be affected by slow diffusion of petroleum ether into a CH_2Cl_2 solution of **4b**: IR ν_{CO}(KBr) 2022 (s), 1973 (s), 1942 (s), 1930 (m), 1797 (m) cm^{-1}; $^{31}P\{^1H\}$ NMR (25 °C, benzene-d_6) δ 211.6 (dd, $J_{^{31}P-^{31}P}$ = 15.8 and 44.4 Hz), 134.9 (ddd, $J_{^{31}P-^{103}Rh}$ = 120.6 Hz, $J_{^{31}P-^{31}P}$ = 206.7 and 18.9 Hz), 115.0 (dddd, $J_{^{31}P-^{103}Rh}$ = 103.7 Hz, $J_{^{31}P-^{31}P}$ = 14.3, 206.7, and 44.4 Hz), 37.8 (dddd, $J_{^{31}P-^{103}Rh}$ = 227.7 Hz, $J_{^{31}P-^{31}P}$ = 15.8, 18.9, and 14.3 Hz).

Preparation of $Fe_2Rh(\mu\text{-}PPh_2)_3(CO)_8$, 5, and $Fe_2Rh(\mu\text{-}PPh_2)_3(CO)_6$, 6. Carbon monoxide was purged through an Et_2O solution (20 mL) of **4b** (0.203 g, 0.169 mmol) for 16 h at 25 °C. The microcrystalline red-purple solid which precipitated during the reaction was filtered under a CO atmosphere and washed with hexane under a CO atmosphere to yield **5** in 79% yield (0.133 g, 0.134 mmol). A CH_2Cl_2 (20 mL) solution of **5** was degassed by five freeze–pump–thaw cycles and the solvent removed in vacuo. The product was extracted into hexane and filtered, and the solvent was evaporated to yield **6** as a green solid.

5: IR ν_{CO}(KBr) 2023 (m), 2008 (vs), 1987 (m), 1975 (s), 1968 (sh, m), 1952 (s) cm^{-1}; $^{31}P\{^1H\}$ NMR (−40 °C, toluene-d_8) δ 110.5 (dd, $J_{^{31}P-^{103}Rh}$ = 91.5 Hz, $J_{^{31}P-^{31}P}$ = 15.3 Hz), 102.6 (t, $J_{^{31}P-^{31}P}$ = 15.3 Hz).

Table I. Data for the X-ray Diffraction Study of $Fe_2Rh(\mu\text{-}PPh_2)(CO)_6(PPh_3)$ (2a)

Crystal Parameters

cryst system: monoclinic
a = 14.062 (9) Å
b = 21.212 (8) Å
c = 19.164 (6) Å
β = 109.22 (4)°
V = 5397 (9) Å
Z = 4
space group: $P2_1/c$
temp = 23 °C
mol wt = 1200.52
d(calcd) = 1.477
μ = 10.888 cm^{-1}, not corrected

Measurement of Intensity Data

radiation: Mo Kα (λ = 0.710 73 Å^{-1})
monochromator: graphite crystal
reflections measured: $+h, +k, \pm l$
data limits: $3° \leqslant 2\theta \leqslant 50°$
unique data: 10 144
nonzero data: 6818 ($I \geqslant 3\sigma(I)$)
std reflections: three measured every 3 h; no significant variation
p = 0.02
R = 0.051; R_w = 0.057

6: IR ν_{CO}(hexane) 2027 (s), 2012 (s), 1997 (s), 1966 (s) cm^{-1}; $^{31}P\{^1H\}$ NMR (−40 °C, toluene-d_8) δ 146.9 (dd, $J_{^{31}P-^{103}Rh}$ = 94.6 Hz, $J_{^{31}P-^{31}P}$ = 23.0 Hz), 65.2 (t, $J_{^{31}P-^{31}P}$ = 23.0 Hz); mass spectrum, *m/e* 938 (M^+), 919 ($M^+ - CO$), 882 ($M^+ - 2CO$), 854 ($M^+ - 3CO$), 826 ($M^+ - 4CO$), 798 ($M^+ - 5CO$), and 770 ($M^+ - 6CO$).

X-ray Structural Analysis of $Fe_2Rh(\mu\text{-}PPh_2)_3(CO)_6(PPh_3)$, 4b. Red crystals of **4b** were grown by slow diffusion of petroleum ether into a saturated CH_2Cl_2 solution of the complex. A crystal measuring 0.25 × 0.35 × 0.35 mm was mounted in an arbitrary orientation on a glass fiber which was then fixed into an aluminum pin and mounted onto a eucentric gonimeter. Diffraction data were collected on a Enraf-Nonius four-circle CAD4 automated diffractometer controlled by a PDP 8a computer. The Enraf-Nonius program SEARCH was employed to obtain 25 accurately centered reflections which were then used in the program INDEX to obtain an orientation matrix for data collection and to provide cell dimensions.[12a] Details of the data collection and reduction procedures have been described previously.[12b] Pertinent crystal and intensity data are listed in Table I.

The Rh, two Fe atoms, four P atoms, 15 C atoms, and three O atoms were located by direct methods using the program MULTAN 78.[12c] The coordinates of the remaining 48 non-hydrogen atoms were determined by successive least-squares refinements and difference Fourier maps. Phenyl hydrogens were fixed with C–H bond lengths of 0.95 Å, C–C–H bond angles of 120°, and isotropic temperature factors of 5.0. The phenyl carbons were refined isotropically, but all other non-hydrogen atoms were refined by using anisotropic temperature factors. After several cycles of least-squares refinement the structure converged with R = 0.051 and R_w = 0.057. The residuals are defined as $R = \sum(||F_o| - |F_c||)/\sum|F_o|$ and $R_w = [\sum w(|F_o| - |F_c|)^2/\sum w|F_o|^2]^{1/2}$. An ORTEP drawing which shows the atom numbering scheme is shown in Figure 2. Final positional and thermal parameters are listed in Tables II and III. Relevant bond distances and bond angles are set out in Tables IV and V. A listing of the observed and calculated structure factors and a table of the derived positions of the phenyl hydrogen atoms are given as supplementary material.

Results

Preparation and Characterization of $Fe_2(\mu\text{-}PPh_2)_2(CO)_{6-x}(PPh_2H)_x$, 1 ($x$ = 1) and 2 (x = 2), and $[Fe_2(\mu\text{-}PPh_2)_2(CO)_5(PPh_2)]^-$, 3. We have previously demonstrated the preparation of phosphido-bridged binuclear Fe–Rh compounds by the reaction of a phosphi-

---

(12) (a) All programs used in this study are part of the Enraf-Nonius Structure Determination Package (SDP), Enraf-Nonius, Delft, Holland, 1975, revised 1977. (b) Steinhardt, P. C.; Gladfelter, W. L.; Harley, A. D.; Fox, J. R.; Geoffroy, G. L. *Inorg. Chem.* **1980**, *19*, 332. (c) Main, P. "Multan 78, A System of Computer Programs for the Automatic Solution of Crystal Structures", Department of Physics, University of York: York, England, 1978; obtained from Dr. Graham J. G. Williams, Brookhaven National Laboratories, Upton, N.Y.

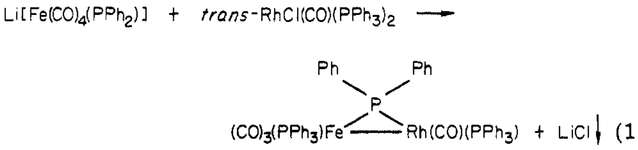

$$\mathrm{Li[Fe(CO)_4(PPh_2)]} + trans\text{-}\mathrm{RhCl(CO)(PPh_3)_2} \longrightarrow \mathrm{(CO)_3(PPh_3)Fe(\mu\text{-}PPh_2)Rh(CO)(PPh_3)} + \mathrm{LiCl}\downarrow \quad (1)$$

dometallate complex with a metal halide, e.g., eq 1.[5] To prepare an Fe_2Rh species with bridging phosphido ligands, we needed the binuclear phosphidometallate $[Fe_2(\mu\text{-}PPh_2)_2(CO)_5(PPh_2)]^-$, **3**. This anion was found to derive by reaction 2, by the sequence of reactions 3 and 4, or by reaction 5 followed by (4). Of these the latter two routes

$$\mathrm{Na_2[Fe_2(\mu\text{-}PPh_2)_2(CO)_6] + PPh_2Cl \xrightarrow[-NaCl]{-CO} Na[Fe_2(\mu\text{-}PPh_2)_2(CO)_5(PPh_2)]} \quad (2)$$

$$\mathrm{Fe_2(\mu\text{-}PPh_2)_2(CO)_6 + PPh_2H \xrightarrow[-CO]{\Delta \text{ or } h\nu} \underset{\mathbf{1}\ (8\text{–}20\%)}{Fe_2(\mu\text{-}PPh_2)_2(CO)_5(PPh_2H)}} \quad (3)$$

$$\mathbf{1} + n\mathrm{BuLi} \xrightarrow[-\mathrm{BuH}]{} \underset{\mathbf{3}}{\mathrm{Li[Fe_2(\mu\text{-}PPh_2)_2(CO)_5(PPh_2)]}} \quad (4)$$

$$\mathrm{[Fe_2(\mu\text{-}PPh_2)_2(CO)_5(PhCO)]^- + H^+ + PPh_2H \rightarrow PhCHO + \underset{\mathbf{1}\ (92\%)}{Fe_2(\mu\text{-}PPh_2)_2(CO)_5(PPh_2H)}} \quad (5)$$

are preferred since the intermediate complex **1** can be purified by chromatography before use. A much better yield of **1** is obtained from reaction 5 as compared to reaction 3. Protonation of the dinuclear acyl complex $[Fe_2(\mu\text{-}PPh_2)_2(CO)_5(PhCO)]^-$ has been reported to yield benzaldehyde,[13] a reaction which also apparently generates the coordinatively unsaturated complex $Fe_2(\mu\text{-}PPh_2)_2(CO)_5$. This latter species must then scavenge PPh_2H to yield **1**. Reaction 4 generates anion **3** in near quantitative yield.

Complex **1** has been characterized spectroscopically and by a satisfactory C, H, and Fe analysis. Its $^{31}P\{^1H\}$ NMR spectrum shows two singlets at δ 145.9 and 51.3 in a 2:1 intensity ratio, consistent with the structure **1**. The downfield $^{31}P\{^1H\}$ NMR resonance is assigned to two equivalent bridging μ-PPh_2 ligands and the upfield resonance to the terminal PPh_2H ligand. Upon ^1H coupling the latter resonance splits into a broad doublet with $J_{^{31}P-^1H} \simeq 360$ Hz. Coupling was not observed between the phosphorus nuclei. The downfield position of the μ-PPh_2 resonance implies the presence of a metal–metal bond in **1**. Numerous correlations have shown that the μ-PR_2 ligands in compounds with metal–metal bonds generally display downfield (δ 50 → 300) ^{31}P NMR resonances whereas upfield (δ 50 → −200) resonances are observed for compounds in which the μ-PR_2 ligand bridges two metals not joined by a metal–metal bond.[7b,14] The mass spectrum of **1** showed a parent ion at m/e 808 with the expected isotropic distribution and fragment ions corresponding to the stepwise loss of the five carbonyl ligands. Compound **1** has been recently described by Collman and co-workers[13] and our IR data for **1** agree with that reported (see Experimental Section).

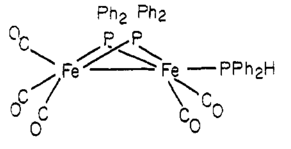

1

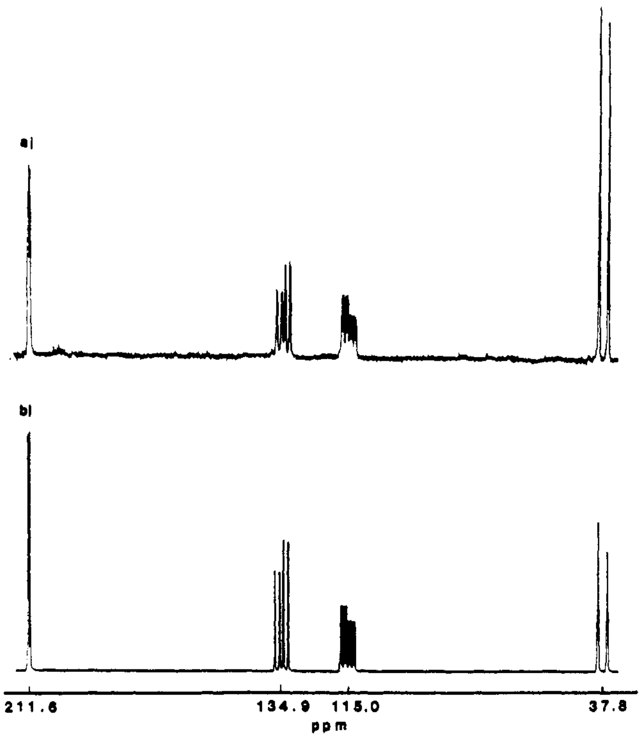

Figure 1. A comparison of the (a) experimental and (b) computer-simulated $^{31}P\{^1H\}$ NMR spectrum of $Fe_2Rh(\mu\text{-}PPh_2)_3(CO)_6(PPh_3)$ (**4b**). The spectrum was recorded at 25 °C in benzene-d_6 solution.

Also isolated from the reaction of $Fe_2(\mu\text{-}PPh_2)_2(CO)_6$ with excess PPh_2H was a small amount (2%) of the disubstituted derivative, $Fe_2(\mu\text{-}PPh_2)_2(CO)_4(PPh_2H)_2$, **2**. The $^{31}P\{^1H\}$ NMR spectrum of this species shows two triplets at δ 135.7 (t) and 54.3 (t) with $J_{^{31}P-^{31}P} = 13.7$ Hz. The δ 135.7 resonance is assigned to two equivalent μ-PPh_2 ligands bridging a metal–metal bond and the δ 54.3 resonance to two equivalent terminal PPh_2H ligands. Structure **2** is implied.

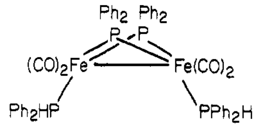

2

The anion **3** is extremely reactive and readily abstracts hydrogen from H_2O to give **1**. All solvents and glassware must be rigorously dried before it can be handled. The IR spectrum of **3** shows the usual shift of the ν_{CO} vibrations to lower energy as compared to **1** (see Experimental Section). The $^{31}P\{^1H\}$ NMR spectrum of **3** shows a triplet at δ 66.5 assignable to the terminal PPh_2 ligand and a doublet at δ 138.1 due to the two equivalent μ-PPh_2 ligands with $J_{^{31}P-^{31}P} = 8.7$ Hz.

Synthesis and Spectroscopic Characterization of $Fe_2Rh(\mu\text{-}PPh_2)_3(CO)_6(PR_3)$, 4. The reaction of **3** with *trans*-$RhCl(CO)(PR_3)_2$ (R = Et, Ph) yields the new complexes $Fe_2Rh(\mu\text{-}PPh_2)_3(CO)_6(PR_3)$, **4a** (R = Et) and **4b** (R = Ph), in good yield (eq 6). These new compounds have

$$\mathbf{3} + trans\text{-}\mathrm{RhCl(CO)(PR_3)_2} \xrightarrow[-\mathrm{LiCl}]{} \mathrm{Fe_2Rh(\mu\text{-}PPh_2)_3(CO)_6(PR_3)} \quad (6)$$
$$\mathbf{4a},\ \mathrm{R = Et}\ (60\%)$$
$$\mathbf{b},\ \mathrm{R = Ph}\ (86\%)$$

been characterized spectroscopically, and **4b** has been

---

[13] Collman, J. P.; Rothrock, R. K.; Finke, R. G.; Moore, E. J.; Ruse-Munch, F. *Inorg. Chem.* **1982**, *21*, 146.

[14] (a) Petersen, J. L.; Stewart, R. P., Jr. *Inorg. Chem.* **1980**, *19*, 186. (b) Carty, A. J.; MacLaughlin, S. A.; Taylor, N. J. *J. Organomet. Chem.* **1981**, *204*, C27. (c) Garrou, P. E. *Chem. Rev.* **1981**, *81*, 229. (d) Johannsen, G.; Stelzer, O. *Chem. Ber.* **1977**, *110*, 3438.

Table II. Positional and Thermal Parameters and Their Estimated Standard Deviations for the Non-Phenyl Atoms of $Fe_2Rh(\mu\text{-}PPh_2)_3(CO)_6(PPh_3)$ (4b)[a]

atom	*x*	*y*	*z*	U_{11}	U_{22}	U_{33}	U_{12}	U_{13}	U_{23}
Rh1	0.32193 (3)	0.47535 (2)	0.23038 (2)	0.0274 (2)	0.0315 (2)	0.0247 (2)	0.0012 (2)	0.0091 (1)	0.0008 (2)
Fe1	0.15269 (5)	0.48445 (4)	0.26597 (4)	0.0350 (4)	0.0502 (5)	0.0385 (4)	0.0072 (4)	0.0185 (3)	0.0104 (4)
Fe2	0.31982 (6)	0.42037 (4)	0.37331 (4)	0.0348 (4)	0.0444 (5)	0.0278 (3)	−0.0008 (4)	0.0085 (3)	0.0013 (4)
P1	0.4040 (1)	0.49543 (7)	0.14711 (7)	0.0349 (6)	0.0338 (7)	0.0298 (6)	0.0014 (6)	0.0136 (5)	0.0009 (6)
P2	0.3805 (1)	0.37942 (7)	0.28305 (7)	0.0318 (7)	0.0346 (8)	0.0309 (6)	0.0011 (6)	0.0086 (5)	0.0031 (6)
P3	0.1538 (1)	0.39470 (8)	0.32426 (7)	0.0337 (7)	0.0508 (9)	0.0316 (6)	−0.0012 (7)	0.0122 (5)	0.0062 (7)
P4	0.2318 (1)	0.56564 (7)	0.22928 (7)	0.0349 (7)	0.0366 (8)	0.0275 (6)	0.0048 (6)	0.0104 (5)	−0.0002 (6)
O1	0.1476 (3)	0.4084 (2)	0.1340 (2)	0.044 (2)	0.060 (3)	0.036 (2)	−0.012 (2)	0.002 (2)	−0.000 (2)
O2	0.2738 (4)	0.4833 (3)	0.4954 (3)	0.090 (3)	0.159 (5)	0.080 (3)	−0.016 (4)	0.043 (2)	−0.065 (3)
O3	0.3950 (4)	0.3077 (2)	0.4610 (2)	0.101 (4)	0.062 (3)	0.059 (2)	0.001 (3)	0.012 (2)	0.032 (2)
O4	−0.0543 (4)	0.4986 (3)	0.1726 (3)	0.038 (3)	0.215 (6)	0.122 (4)	0.026 (3)	0.017 (3)	0.069 (4)
O5	0.4885 (3)	0.5112 (2)	0.4135 (2)	0.061 (2)	0.070 (3)	0.049 (2)	−0.023 (2)	0.012 (2)	−0.009 (2)
O6	0.1242 (4)	0.5680 (3)	0.3781 (3)	0.247 (4)	0.076 (4)	0.143 (3)	0.032 (3)	0.162 (2)	0.003 (3)
C1	0.1818 (4)	0.4396 (3)	0.1865 (3)	0.030 (3)	0.048 (3)	0.032 (2)	−0.001 (3)	0.006 (2)	0.012 (3)
C2	0.2858 (5)	0.4596 (3)	0.4454 (3)	0.044 (3)	0.081 (5)	0.059 (3)	−0.011 (3)	0.016 (3)	−0.023 (3)
C3	0.3669 (4)	0.3519 (3)	0.4263 (3)	0.047 (3)	0.062 (4)	0.035 (3)	−0.006 (3)	0.008 (2)	0.002 (3)
C4	0.0276 (5)	0.4930 (4)	0.2098 (4)	0.049 (3)	0.098 (5)	0.072 (4)	0.014 (4)	0.033 (2)	0.032 (4)
C5	0.4244 (4)	0.4755 (3)	0.3940 (3)	0.046 (3)	0.049 (3)	0.032 (3)	0.007 (3)	0.009 (2)	0.002 (3)
C6	0.1365 (5)	0.5341 (3)	0.3363 (3)	0.110 (4)	0.056 (4)	0.087 (3)	0.021 (3)	0.077 (2)	0.021 (3)

[a] The form of the anisotropic thermal parameter is $\exp[-2\pi^2(U_{11}h^2a^{*2} + U_{22}k^2b^{*2} + U_{33}l^2c^{*2} + 2U_{12}hka^*b^* + 2U_{13}hla^*c^* + 2U_{23}klb^*c^*)]$.

Table III. Positional and Isotropic Thermal Parameters and Their Standard Deviations for the Phenyl Carbon Atoms of $Fe_2Rh(\mu\text{-}PPh_2)(CO)_6(PPh_3)$ (4b)

atom	*x*	*y*	*z*	*B*, Å^2	atom	*x*	*y*	*z*	*B*, Å^2
C110	0.3797 (4)	0.4362 (3)	0.0733 (3)	2.9 (1)	C223	0.3032 (5)	0.1852 (3)	0.1703 (4)	5.3 (2)
C111	0.4551 (4)	0.4010 (3)	0.0591 (3)	3.7 (1)	C224	0.3436 (5)	0.1889 (3)	0.2454 (4)	5.0 (2)
C112	0.4279 (5)	0.3562 (3)	0.0019 (4)	4.7 (1)	C225	0.3628 (5)	0.2470 (3)	0.2808 (3)	4.3 (1)
C113	0.3309 (5)	0.3465 (3)	−0.0387 (4)	5.0 (1)	C310	0.1104 (4)	0.3198 (3)	0.2779 (3)	3.8 (1)
C114	0.2537 (5)	0.3809 (3)	−0.0249 (3)	4.6 (1)	C311	0.1434 (6)	0.2638 (4)	0.3100 (4)	6.2 (2)
C115	0.2790 (4)	0.4266 (3)	0.0315 (3)	3.6 (1)	C312	0.1078 (7)	0.2056 (4)	0.2746 (5)	8.0 (2)
C120	0.5412 (4)	0.5038 (3)	0.1865 (3)	2.9 (1)	C313	0.0418 (6)	0.2062 (4)	0.2080 (5)	7.5 (2)
C121	0.5860 (4)	0.5011 (3)	0.2632 (3)	3.4 (1)	C314	0.0055 (6)	0.2585 (4)	0.1743 (4)	7.4 (2)
C122	0.6894 (4)	0.5101 (3)	0.2963 (3)	4.0 (1)	C315	0.0378 (6)	0.3181 (4)	0.2075 (4)	6.1 (2)
C123	0.7492 (5)	0.5199 (3)	0.2519 (3)	4.9 (1)	C320	0.0856 (4)	0.3924 (3)	0.3921 (3)	3.5 (1)
C124	0.7064 (5)	0.5227 (3)	0.1764 (4)	4.9 (1)	C321	−0.0008 (5)	0.4278 (3)	0.3816 (4)	5.4 (2)
C125	0.6030 (4)	0.5156 (3)	0.1437 (3)	3.9 (1)	C322	−0.0501 (6)	0.4282 (4)	0.4335 (4)	6.2 (2)
C130	0.3725 (4)	0.5707 (3)	0.0966 (3)	2.9 (1)	C323	−0.0164 (5)	0.3929 (3)	0.4952 (4)	5.5 (2)
C131	0.4063 (4)	0.6253 (3)	0.1371 (3)	3.7 (1)	C324	0.0667 (6)	0.3569 (4)	0.5064 (4)	6.4 (2)
C132	0.3785 (5)	0.6844 (3)	0.1050 (3)	4.8 (1)	C325	0.1193 (5)	0.3569 (3)	0.4547 (4)	5.4 (2)
C133	0.3195 (5)	0.6889 (3)	0.0335 (4)	5.3 (2)	C410	0.1536 (4)	0.6057 (3)	0.1459 (3)	3.0 (1)
C134	0.2883 (5)	0.6368 (3)	−0.0087 (4)	5.5 (2)	C411	0.1000 (5)	0.5699 (3)	0.0850 (3)	4.2 (1)
C135	0.3150 (5)	0.5761 (3)	0.0229 (3)	4.2 (1)	C412	0.0358 (5)	0.5966 (3)	0.0209 (4)	5.3 (2)
C210	0.5173 (4)	0.3633 (3)	0.3154 (3)	3.1 (1)	C413	0.0207 (5)	0.6609 (3)	0.0167 (4)	5.2 (2)
C211	0.5813 (4)	0.3704 (3)	0.3877 (3)	3.8 (1)	C414	0.0737 (6)	0.6975 (4)	0.0746 (4)	6.4 (2)
C212	0.6859 (5)	0.3587 (3)	0.4066 (4)	5.1 (2)	C415	0.1430 (5)	0.6704 (3)	0.1387 (4)	5.1 (2)
C213	0.7227 (6)	0.3399 (4)	0.3543 (4)	5.8 (2)	C420	0.2890 (4)	0.6289 (3)	0.2935 (3)	3.1 (1)
C214	0.6625 (5)	0.3312 (3)	0.2826 (4)	5.4 (2)	C421	0.2304 (5)	0.6734 (3)	0.3149 (3)	4.9 (1)
C215	0.5592 (5)	0.3429 (3)	0.2623 (3)	4.2 (1)	C422	0.2773 (6)	0.7221 (4)	0.3632 (4)	6.2 (2)
C220	0.3407 (4)	0.3027 (3)	0.2398 (3)	2.9 (1)	C423	0.3803 (6)	0.7246 (4)	0.3893 (4)	6.8 (2)
C221	0.2995 (5)	0.2983 (3)	0.1631 (3)	4.1 (1)	C424	0.4384 (6)	0.6830 (4)	0.3693 (4)	5.9 (2)
C222	0.2822 (5)	0.2394 (3)	0.1283 (4)	5.3 (2)	C425	0.3931 (5)	0.6333 (3)	0.3207 (3)	4.0 (1)

characterized by a complete single-crystal X-ray diffraction study (vide infra) which showed the triangular structure sketched below. The $^{31}P\{^1H\}$ NMR spectra of both **4a** and

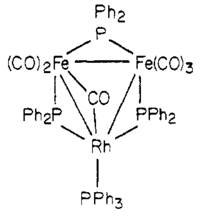

4b

4b are consistent with the solid-state structure. A comparison of the experimental and computer-simulated $^{31}P\{^1H\}$ NMR spectrum of **4b** is shown in Figure 1. It shows resonances at δ 211.6 (dd), 134.9 (ddd), 115.0 (dddd), and 37.8 (dddd). The resonance at δ 37.8 is assigned to the terminal PPh_3 ligand attached to Rh. It shows large ^{31}P–^{103}Rh coupling (227.7 Hz) and is in the region normally observed for PPh_3 ligands attached to Rh(I) (e.g., *trans*-$RhCl(CO)(PPh_3)_2$, δ 28.8 (d)). This phosphorus also couples to the three μ-PPh_2 ligands, with the specific coupling constants given in the Experimental Section. The resonances at δ 134.9 and 115.0 also show strong ^{31}P–^{103}Rh coupling of 120.6 and 103.7 Hz, respectively. These resonances are thus assigned to the two inequivalent μ-PPh_2 ligands which bridge the FeRh bonds. The δ 115.0 resonance shows coupling to all the other ^{31}P nuclei present, but the δ 134.9 resonance exhibits coupling only to the other FeRh(μ-PPh_2) bridge and to the PPh_3 on Rh. The δ 211.6 resonance does not show ^{103}R–^{31}P coupling and is assigned to the μ-PPh_2 ligand which bridges the Fe–Fe bond. Surprisingly, this phosphorus weakly couples to the PPh_3 bound to Rh ($J_{^{31}P-^{31}P}$ = 15.8 Hz) even though it does not couple to the Rh nucleus itself. It also couples to one

Table IV. Selected Bond Distances (Å) in $Fe_2Rh(\mu\text{-}PPh_2)_3(CO)_6(PPh_3)$

	Metal–Metal		
Fe1–Fe2	2.901 (1)	Fe2–Rh1	2.986 (1)
Fe1–Rh1	2.690 (1)		
	Metal–Phosphorus		
Fe1–P3	2.205 (1)	Rh1–P1	2.296 (1)
Fe1–P4	2.283 (1)	Rh1–P2	2.300 (1)
Fe2–P2	2.334 (1)	Rh1–P4	2.293 (1)
Fe2–P3	2.277 (1)		
	Metal–Carbon		
Fe1–C1	1.940 (4)	Fe2–C3	1.770 (4)
Fe1–C4	1.743 (5)	Fe2–C5	1.817 (4)
Fe1–C6	1.784 (5)	Rh1–C1	2.018 (3)
Fe2–C2	1.808 (4)		
	Carbon–Oxygen		
C1–O1	1.169 (4)	C4–O4	1.143 (5)
C2–O2	1.142 (5)	C5–O5	1.143 (4)
C3–O3	1.141 (4)	C6–O6	1.130 (5)

Table V. Selected Bond Angles (Deg) in $Fe_2Rh(\mu\text{-}PPh_2)_3(CO)_6(PPh_3)$ (4b)

	M–M–M		
Fe1–Rh1–Fe2	61.22 (1)	Rh1–Fe1–Fe2	64.43 (2)
Fe1–Fe2–Rh1	54.35 (1)		
	M–P–M		
Rh1–P2–Fe1	80.24 (3)	Fe1–P3–Fe2	80.67 (4)
Rh1–P4–Fe1	72.00 (3)		
	P–M–P		
P1–Rh1–P2	106.24 (3)	P3–Fe1–P4	152.19 (4)
P1–Rh1–P4	103.98 (3)	P2–Fe2–P3	100.39 (4)
P2–Rh1–P4	149.31 (3)		
	M–M–P		
Fe2–Fe1–P3	50.75 (3)	Fe1–Fe2–P3	48.58 (3)
Fe2–Fe1–P4	102.05 (3)	Fe1–Rh1–P1	148.44 (3)
Rh1–Fe1–P3	101.96 (3)	Fe1–Rh1–P2	99.85 (3)
Rh1–Fe1–P4	54.18 (2)	Fe1–Rh1–P4	53.82 (3)
Rh1–Fe2–P2	49.39 (2)	Fe2–Rh1–P1	150.33 (3)
Rh1–Fe2–P3	91.90 (3)	Fe2–Rh1–P2	50.37 (2)
Fe1–Fe2–P2	93.29 (3)	Fe2–Rh1–P4	99.33 (2)
	P–M–C		
P1–Rh1–C1	115.19 (10)	P4–Fe1–C6	89.08 (14)
P2–Rh1–C1	90.58 (10)	P2–Fe2–C2	172.53 (13)
P4–Rh1–C1	81.29 (10)	P2–Fe2–C3	87.78 (13)
P3–Fe1–C1	90.37 (10)	P2–Fe2–C5	86.19 (11)
P3–Fe1–C4	103.91 (15)	P3–Fe2–C2	86.11 (13)
P3–Fe1–C6	96.20 (13)	P3–Fe2–C3	100.34 (13)
P4–Fe1–C1	83.01 (10)	P3–Fe2–C5	152.87 (12)
P4–Fe1–C4	103.05 (15)		
	M–M–C		
Fe2–Fe1–C1	89.76 (9)	Rh1–Fe2–C3	137.04 (13)
Fe2–Fe1–C4	154.65 (15)	Rh1–Fe2–C5	72.35 (11)
Fe2–Fe1–C6	90.90 (16)	Fe1–Fe2–C2	88.25 (14)
Rh1–Fe1–C1	48.39 (10)	Fe1–Fe2–C3	148.58 (12)
Rh1–Fe1–C4	130.41 (14)	Fe1–Fe2–C5	105.17 (11)
Rh1–Fe1–C6	125.30 (16)	Fe1–Rh1–C1	46.25 (10)
Rh1–Fe2–C2	127.32 (15)	Fe2–Rh1–C1	86.11 (9)
	M–C–O		
Rh1–C1–O1	129.81 (28)	Fe2–C2–O2	173.18 (40)
Fe1–C1–O1	144.76 (28)	Fe2–C3–O3	178.21 (38)
Fe1–C4–O4	179.51 (48)	Fe2–C5–O5	173.11 (31)
Fe1–C6–O6	176.28 (43)		

of the μ-PPh_2 ligands which bridges an Fe–Rh bond. The $^{31}P\{^1H\}$ NMR spectrum of **4a** (see Experimental Section) is similar to that of **4b**, and analogous assignments are appropriate.

The IR spectra of **4a** and **4b** show bands at 1781 and 1797 cm^{-1};, respectively, which are attributed to the bridging carbonyl shown by the X-ray structure of **4b**. The overall similarity of the IR spectra of **4a** and **4b** (see the Experimental Section) strongly argues for similar structures for the two complexes.

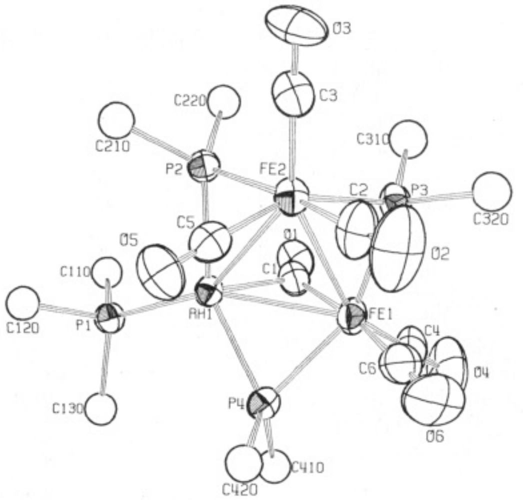

Figure 2. An ORTEP plot of the molecular structure of $Fe_2Rh(\mu\text{-}PPh_2)_3(CO)_6(PPh_3)$ (**4b**). Thermal ellipsoids are drawn at the 50% probability level. Only the carbon atoms directly bonded to phosphorus from the phenyl groups are shown.

Both **4a** and **4b** are air-stable in the solid state but slowly decompose in solutions exposed to air. Solutions of **4b** maintained at 25 °C under N_2 appear to be stable for prolonged periods but the complex decomposes over a several hour period when heated to 60 °C. Complex **4a** decomposes even at 25 °C in solutions under N_2, and ^{31}P NMR spectra indicate complete decomposition within 24 h. The ^{31}P NMR changes are quite complex for the decomposition of both **4a** and **4b**, indicating the formation of multiple products, but these have not been identified.

Crystal and Molecular Structure of $Fe_2Rh(\mu\text{-}PPh_2)_3(CO)_6(PPh_3)$, 4b. An ORTEP plot of the structure of $Fe_2Rh(\mu\text{-}PPh_2)_3(CO)_6(PPh_3)$ is shown in Figure 2. It consists of a triangular arrangement of the metal atoms with a single μ-PPh_2 ligand bridging each of the metal pairs. Fe2 is further ligated by three CO's, Fe1 by two CO's, and Rh by the PPh_3 ligand. In addition, one carbonyl bridges the Fe1–Rh bond. The μ-PPh_2 ligands are arranged such that P1(PPh_3) is only 0.018 Å above the Fe_2Rh plane, P2 and P3 lie 1.248 and 1.239 Å, respectively, above the Fe_2Rh plane, and P4 lies 1.438 Å below the plane. This arrangement of μ-PPh_2 ligands differs from that commonly observed in $M_3(\mu\text{-}PR_2)_3$ structures where one phosphorus generally lies in the M_3 plane, one above, and one below.[15]

The Fe1–Rh bond length of 2.690 (1) Å compares well with the μ-PPh_2-bridged FeRh bond lengths in $[Rh\{Fe(\mu\text{-}PPh_2)(CO)_2(\eta^5\text{-}CH_3C_5H_4)\}_2]^+$ (2.659 (2), 2.675 (2) Å[16] and $Rh_2Fe_2(\mu\text{-}PPh_2)_4(CO)_8$ (2.623 Å).[17] However, it is substantially longer than the unbridged FeRh bonds in $Fe_2Rh_2(\eta^5\text{-}C_5H_5)_2(CO)_8$ (2.570 (5), 2.598 (5), 2.598 (5) Å)[18] and $Fe_3Rh(\eta^5\text{-}C_5H_5)(CO)_{11}$ (2.568 (3), 2.615 (3), 2.607 (3) Å).[19] The Fe1–Fe2 and Fe2–Rh bond lengths of 2.901 (1)

---

(15) (a) Huntsman, J. R. Ph.D. Thesis, University of Wisconsin, Madison, 1973. (b) Keller, E.; Vahrenkamp, H. *J. Organomet. Chem.* **1978**, *155*, C41. (c) Billing, E.; Jamerson, J. D.; Pruett, R. T. *Ibid.* **1980**, *192*, C49.

(16) Mason, R.; Zubieta, J. A. *J. Organomet. Chem.* **1974**, *66*, 279.

(17) Haines, R. J.; Steen, N. D. C. T.; English, R. B. *J. Chem. Soc., Chem. Commun.* **1981**, 587.

(18) Churchill, M. R.; Veidis, M. V. *J. Chem. Soc. A* **1971**, 2170.

(19) Churchill, M. R.; Veidis, M. V. *J. Chem. Soc., Chem. Commun.* **1970**, 1470.

Å and 2.986 (1) Å, respectively, are much longer than expected for direct single metal–metal bonds but do imply some degree of metal–metal interaction. All metal–phosphorus bond lengths and M–P–M bond angles fall within the ranges found in other Fe–Rh phosphido-bridged compounds.[15c,16,17,20–23]

Reactivity of $Fe_2Rh(\mu\text{-}PPh_2)_3(CO)_6(PR_3)$. When solutions of either **4a** or **4b** are stirred at 25 °C under 1 atm of carbon monoxide, a rapid (~5 min) color change from green to red occurs and a red-purple precipitate deposits. This latter material can be isolated in >70% yield. The complex has proven too unstable to obtain a satisfactory elemental analysis, but its spectroscopic properties imply the formulation $Fe_2Rh(\mu\text{-}PPh_2)_3(CO)_8$, **5**. The reaction shown in eq 7, in which two CO's add with concomitant displacement of the PR_3 ligand, is thus indicated. When

$$\underset{\mathbf{4}}{Fe_2Rh(\mu\text{-}PPh_2)_3(CO)_6(PR_3)} + 2CO \rightleftharpoons \underset{\mathbf{5}}{Fe_2Rh(\mu\text{-}PPh_2)_3(CO)_8} + PR_3 \quad (7)$$

the reaction is monitored by ^{31}P NMR spectroscopy, the characteristic signals of PEt_3 (δ -17.7) and PPh_3 (δ -6.0) respectively appear as **4a** and **4b** react. As indicated in eq 6, these CO addition/PR_3 displacement reactions are reversible. When PPh_3 and PEt_3 are added to solutions of **5**, complexes **4a** and **4b** respectively reform, as long as the released CO is removed by an N_2 purge or the solvent evaporated under reduced pressure.

The -40 °C $^{31}P\{^1H\}$ NMR spectrum of **5** shows two resonances at δ 110.5 (dd, $J_{^{31}P-^{103}Rh}$ = 91.5 Hz, $J_{^{31}P-^{31}P}$ = 15.3 Hz) and 102.6 (t, $J_{^{31}P-^{31}P}$ = 15.3 Hz) in a 2:1 intensity ratio, indicating a structure with two equivalent μ-PPh_2 ligands which are attached to Rh and one inequivalent μ-PPh_2 ligand not bound to Rh. Its IR spectrum shows only terminal ν_{CO} bands (see Experimental Section). The -80 °C natural abundance ^{13}C NMR spectrum of **5** shows resonances at δ 217.0 (dd, $J_{^{31}P-^{13}C}$ = 4.9 and 2.9 Hz), 202.2 (t, $J_{^{31}P-^{13}C}$ = 10.8 Hz), 201.8 (t, $J_{^{31}P-^{13}C}$ = 10.0 Hz), and 196.0 (d of t, $J_{^{103}Rh-^{13}C}$ = 79.8 Hz, $J_{^{31}P-^{13}C}$ = 10.8 Hz). These integrate in an approximate 1:1:1:1 intensity ratio with only the δ 196.0 resonance showing ^{13}C–^{103}Rh coupling. This data thus imply that two CO's are attached to Rh and six are terminally bound to the Fe atoms, and the structure sketched below is suggested.

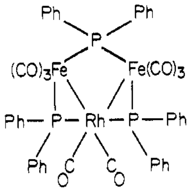

5

Complex **5** has 50 valence electrons and thus a triangular structure such as that shown requires only 2 metal-metal bonds. A conversion similar to **4** → **5** has been observed by Carty and co-workers[14b,24] in which addition of CO to $Ru_3(CO)_8(C{\equiv}C\text{-}i\text{-}Pr)(\mu\text{-}PPh_2)$ causes rupture of the phosphido-bridged Ru–Ru bond but leaves the triangular structure intact. Complex **5** is also isoelectronic with $Fe_2Co(\mu\text{-}PMe_2)(\mu\text{-}SMe)_2(CO)_5$ which has been shown by X-ray diffraction to adopt a structure similar to that drawn with the PMe_2 ligand bridging two nonbonded Fe atoms and with two CO's bound to Co and three to each of the two Fe's.[25]

In the absence of excess PR_3 ligand, freeze–pump–thaw cycles of solutions of **5** removes CO and the new complex $Fe_2Rh(\mu\text{-}PPh_2)_3(CO)_6$ forms. Quantitative analysis of the gas removed in the **5** → **6** conversion shows an average of 2.1 equiv of gas obtained/mol of **5**, implying the loss of two CO's (eq 8). This CO elimination reaction is reversible

$$\underset{\mathbf{5}}{Fe_2Rh(\mu\text{-}PPh_2)_3(CO)_8} \xrightleftharpoons[\text{1 atm of CO}]{\text{evac}} 2CO + \underset{\mathbf{6}}{Fe_2Rh(\mu\text{-}PPh_2)_3(CO)_6} \quad (8)$$

since complex **5** immediately reforms when solutions of **6** are exposed to 1 atm of CO at 25 °C. The mass spectrum of **6** shows the expected parent ion at *m/e* 938 and fragment ions corresponding to the loss of six CO's. Its $^{31}P\{^1H\}$ NMR spectrum shows two resonances in an approximate 2:1 intensity ratio at δ 146.9 (dd, $J_{^{31}P-^{103}Rh}$ = 94.6 Hz, $J_{^{31}P-^{31}P}$ 23.0 Hz) and 65.2 (t, $J_{^{31}P-^{31}P}$ = 23.0 Hz), implying two μ-PPh_2 ligands bridging Fe–Rh bonds and one μ-PPh_2 ligand bridging an Fe–Fe bond. The natural abundance ^{13}C NMR spectrum of **6** at -60 °C shows three resonances at δ 215.8 (d, $J_{^{31}P-^{13}C}$ = 5.9 Hz), 204.5 (t, $J_{^{31}P-^{13}C}$ = 13.3 Hz), and 204.1 (t, $J_{^{31}P-^{13}C}$ = 13.3 Hz). None of these resonances show ^{13}C–^{103}Rh coupling. The spectroscopic data thus imply the structure sketched below for **6**, in which three carbonyls are attached to each Fe atom but with none bound to Rh.

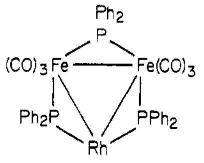

6

$Fe_2Rh(\mu\text{-}PPh_2)_3(CO)_8$, **5**, shows no noticable decomposition when stirred under 1 atm of CO at 40 °C for several days, although it does slowly decompose to several unidentified products when left in solution under N_2 at 25 °C. The hexacarbonyl cluster $Fe_2Rh(\mu\text{-}PPh_2)_3(CO)_6$, **6**, is the least stable of all the complexes reported herein, decomposing in solutions at 25 °C under N_2 with a half-life of about 30 min.

Discussion

The new cluster complexes $Fe_2Rh(\mu\text{-}PPh_2)_3(CO)_6(PR_3)$ (**4a** (R = Et) and **4b** (R = Ph)), $Fe_2Rh(\mu\text{-}PPh_2)_3(CO)_8$, and $Fe_2Rh(\mu\text{-}PPh_2)_3(CO)_6$ have been prepared and characterized spectroscopically, and **4b** has been characterized by a complete single-crystal X-ray diffraction study. The latter showed the cluster to have the closed triangular structure depicted in Figure 2. However, the open structure drawn below is also consistent with the $^{31}P\{^1H\}$ NMR

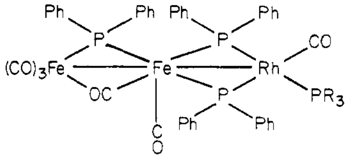

and IR spectra of **4b** in that it possesses a bridging CO and has two μ-PPh_2 ligands bridging an Fe–Rh bond and one μ-PPh_2 ligand bridging two Fe atoms. It is, of course, not

---

(20) Kreter, P. E.; Meek, D. W.; Christoph, G. G. *J. Organomet. Chem.* **1980**, *188*, C27.

(21) Haines, R. J.; Steen, N. D. C. T.; Laing, M.; Sommerville, P. *J. Organomet. Chem.* **1980**, *198*, C72.

(22) Jamerson, J. C.; Pruett, R. L.; Billig, E.; Fiato, F. A. *J. Organomet. Chem.* **1980**, *193*, C43.

(23) (a) Haines, R. J.; Steen, N. D. C. T.; English, R. B. *J. Chem. Soc., Chem. Commun.* **1981**, 407. (b) Haines, R. J.; Steen, N. D. C. T.; English, R. B. *J. Organomet. Chem.* **1981**, *209*, C34.

(24) Carty, A. J. *Pure Appl. Chem.* **1982**, *54*, 113.

(25) Keller, E.; Vahrenkamp, H. *Chem. Ber.* **1981**, *114*, 1111.

the structure of **4b** determined by X-ray diffraction, but an equilibrium between the closed and open forms with the open form existing in solution but rearranging to the closed form upon crystallization cannot be excluded by the present data. In the closed form the cluster is electron sufficient with 48 electrons, whereas the open form is deficient by two electrons. However it contains Rh, a metal which forms a large number of 16-valence-electron complexes. Open structures have been determined for the 48-electron complex $[Fe_2Rh(\mu\text{-}PPh_2)_2(CO)_2(\eta^5\text{-}CH_3C_5H_4)_2]^+$ and its derivatives, but in these complexes Rh lies between the Fe atoms.[16,26] Analogous Fe–Rh–Fe arrangements for **4a** and **4b** would not be consistent with their spectroscopic data since each clearly possesses a μ-PPh_2 ligand that is not bound to Rh and consequently bridges two Fe atoms. An equilibrium between open and closed forms of **4a** and **4b** would require rearrangement of the bridging μ-PPh_2 ligands, but such rearrangement obviously occurs during the synthesis of the compounds and is also known to occur with other phosphido-bridged compounds.[7a,17,20,21,23,27]

Likewise, an open structure such as that sketched in **7** could be considered for $Fe_2Rh(\mu\text{-}PPh_2)_3(CO)_8$. This structure has two μ-PPh_2 ligands attached to Rh and one which is not, consistent with the ^{31}P NMR data. However, if structure **7** did exist in solution, two of the CO's should appear as a doublet of triplets in the ^{13}C NMR spectrum of $Fe_2Rh(\mu\text{-}PPh_2)_3(CO)_8$. However, no such pattern was observed, and thus structure **7** is not indicated.

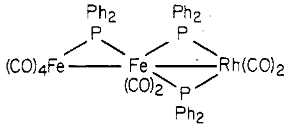

7

Although this research did lead to the preparation of phosphido-bridged clusters containing a Rh(I) center, these particular compounds are not suitable for detailed reactivity studies because of their relative instability. None of the Fe_2Rh species reported herein are stable in solution above 65 °C, and **4a**, **5**, and **6** slowly decompose in solutions maintained at 25 °C. Clearly, the bridging phosphido ligands are not sufficient to maintain structural integrity in these particular Fe_2Rh complexes and other metal–ligand combinations will have to be sought.

Acknowledgment. This research was supported by the National Science Foundation (Grant CHE-8201160). G.L.G. gratefully acknowledges the Camille and Henry Dreyfus Foundation for a Teacher-Scholar Award (1978–1983).

Registry No. 1, 79172-58-0; **2**, 83043-70-3; **3**, 83043-71-4; **4a**, 83043-72-5; **4b**, 83043-73-6; **5**, 83060-54-2; **6**, 83043-74-7; $Na_2[Fe_2(\mu\text{-}PPh_2)_2(CO)_6]$, 64883-57-4; $Fe_2(\mu\text{-}PPh_2)_2(CO)_6$, 19599-68-9; *trans*-$RhCl(CO)(PEt_3)_2$, 15631-52-4; *trans*-$RhCl(CO)(PPh_3)_2$, 15318-33-9; PPh_2Cl, 1079-66-9; PhLi, 591-51-5; PPh_2H, 829-85-6; CO, 630-08-0; Fe, 7439-89-6; Rh, 7440-16-6.

Supplementary Material Available: Listings of the derived positions of the phenyl hydrogen atoms (Table A) and the structure factors for $Fe_2Rh(\mu\text{-}PPh_2)_3(CO)_6(PPh_3)$ (Table B) (51 pages). Ordering information is given on any current masthead page.

---

[26] Burckett-St. Laurent, J. C. T. R.; Haines, R. J.; Nolte, C. R.; Steen, N. D. C. T. *Inorg. Chem.* **1980**, *19*, 577.

[27] Harley, A. D.; Geoffroy, G. L. *Organometallics*, in press.

Phosphazenes with Olefinic Side Groups: Proton Abstraction Reactions of Fluoroalkoxy Derivatives

Harry R. Allcock,* Paul R. Suszko, and Thomas L. Evans

Department of Chemistry, The Pennsylvania State University, University Park, Pennsylvania 16802

Received April 28, 1982

The cyclic phosphazenes $N_3P_3(OPh)_5OCH_2CF_3$, $[NP(OPh)(OCH_2CF_3)]_3$, and $[NP(OCH_2CF_3)_2]_3$ undergo dehydrofluorination and deprotonation when treated with *n*-butyllithium at −78 °C to form metalated intermediates of formula $N_3P_3(OPh)_5OC(Li){=}CF_2$, $[NP(OPh)(OC(Li){=}CF_2)]_3$, and $[NP(OC(Li){=}CF_2)_2]_3$, respectively. These species are stable in solution at −78 °C but react with electrophiles such as 2-propanol, 2-propanol-*d*, methyl iodide, or triphenyltin chloride to yield the cyclophosphazenes with $-OC(H){=}CF_2$, $-OC(D){=}CF_2$, $-OC(CH_3){=}CF_2$, or $-OC(SnPh_3){=}CF_2$ side groups. The reactions were monitored by the use of ^{19}F NMR spectroscopy. A reaction mechanism is proposed. Comparisons are made with the reactions between *n*-butyllithium and trifluoroethoxy-substituted cyclic tetrameric and high polymeric phosphazenes.

The synthesis and properties of many (fluoroalkoxy)phosphazene compounds have been described in recent years.[1-6] The simplest species of this type (such as **1**, **2**, or **3**) can be obtained by the reaction of sodium trifluoroethoxide with hexachlorocyclotriphosphazene, $(NPCl_2)_3$.[4] Moreover, high polymeric analogues are accessible via the interaction of sodium trifluoroethoxide with poly(dichlorophosphazene), $(NPCl_2)_n$.[7,8] High polymers

---

[1] See, for example: Allcock, H. R. "Phosphorus-Nitrogen Compounds"; Academic Press: New York, 1972; Chapter 6, p 16.

[2] McBee, E. T.; Allcock, H. R.; Caputo, R.; Kalmus, A.; Roberts, C. W. *U.S. Gov. Res. Dev. Rep.* **1959**, AD 209,669.

[3] Ratz, R.; Schroeder, H.; Ulrich, H.; Kober, E.; Grundmann, C. *J. Am. Chem. Soc.* **1962**, *84*, 551.

[4] Allcock, H. R.; Schmutz, J. L.; Kosydar, K. M. *Macromolecules* **1978**, *11*, 179.

[5] Heatley, F.; Todd, S. M. *J. Chem. Soc. A* **1966**, 1152.

[6] Gol'din, G. S.; Federov, S. G.; Zapuskalova, S. F.; Naumov, A. D. *Zh. Obsch. Khim.* **1976**, *46*, 688.

[7] Allcock, H. R.; Kugel, R. L. *J. Am. Chem. Soc.* **1965**, *87*, 4216.

[8] Allcock, H. R.; Kugel, R. L.; Valan, K. J. *Inorg. Chem.* **1966**, *5*, 1709.

0276-7333/82/2301-1443$01.25/0